# Non-Local Form Factors from Lattice QCD

Chris Sachrajda
University of Southampton

*Beyond the Flavour Anomalies 2025*
*Rome, 9th-11th April 2025*

University of Southampton

# 1. Introduction

- At this workshop, it is not necessary for me to underline that processes mediated by FCNC, which are rare in the SM, are a fruitful area for exploring the limits of the SM and in searching for signatures of New Physics.

- In order to compute the full amplitudes for decays such as $B \to K\ell^+\ell^-$ and $B_s \to \gamma\ell^+\ell^-$ using lattice QCD, in addition to controlling the usual lattice systematic uncertainties (e.g. continuum, finite-volume, heavy-quark mass extrapolations), we must handle the new difficulties present in the Minkowski →Euclidean space continuation.

    - The new difficulties arise because the amplitudes are complex.

    - New methods, based on the spectral density approach, have and are being developed to tackle this problem.

    - The methods can be applied, in particular (but not only) to the “charming penguin” contributions.

# Introduction (cont.)

- Much of the presentation will be based on:

  - "$B_s \to \mu^+\mu^-\gamma$ decay rates at large $q^2$ from lattice QCD",
    R.Frezzotti, G.Gagliardi, V.Lubicz, G.Martinelli, CTS, F.Sanfilippo, S.Simula and N.Tantalo, arXiv:2402.03262

  - "Theoretical framework for lattice QCD computations of $B \to K\ell^+\ell^-$ and $B_s \to \gamma\ell^+\ell^-$ decay rates, including contributions from "Charming Penguins",
    R.Frezzotti, G.Gagliardi, V.Lubicz, G.Martinelli, CTS, F.Sanfilippo, S.Simula and L.Silvestrini (in preparation)

  which in turn are based on papers including:

  - **HLT -** "Extraction of spectral densities from lattice correlators",
    M.Hansen, A.Lupo and N.Tantalo, arXiv:1903.06476

  - **SFR -** "Spectral function determination of complex electroweak amplitudes with lattice QCD",
    R.Frezzotti, G.Gagliardi, V.Lubicz, F.Sanfilippo, S.Simula and N.Tantalo, arXiv:2402.03262
    **SFR** = Spectral Function Reconstruction.

I warmly thank my collaborators from whom I learned much of the material presented in this talk.

# Outline

1. Introduction.
2. Motivation for introducing the spectral density approach.
3. The $\bar{B}_s \to \gamma\mu^+\mu^-$ decay rate at large $q^2$.
4. Towards the evaluation of the charming penguin contributions.
5. Other contributions requiring spectral density methods.
6. Renormalisation
7. Conclusions.
8. Giuseppe Gagliardi report on the status of the exploratory numerical calculations.

# The Effective b → s Hamiltonian

$$\mathscr{H}_{\text{eff}}^{b\to s} = 2\sqrt{2} G_F V_{tb} V_{ts}^* \left[ \sum_{i=1,2} C_i O_i^c + \sum_{i=3}^{6} C_i O_i + \frac{\alpha_{\text{em}}}{4\pi} \sum_{i=7}^{10} C_i O_i \right]$$

$$O_1^c = (\bar{s}_i \gamma^\mu P_L c_j)\ (\bar{c}_j \gamma_\mu P_L b_i) \qquad O_2^c = (\bar{s} \gamma^\mu P_L c)\ (\bar{c} \gamma_\mu P_L b)$$

$$\left( P_{L,R} = \frac{1}{2}(1 \mp \gamma^5) \right)$$

$O_{3-6}$ are QCD Penguins with small Wilson Coefficients

$$O_7 = -\frac{m_b}{e} (\bar{s} \sigma^{\mu\nu} F_{\mu\nu} P_R b) \qquad O_8 = -\frac{g_s m_b}{4\pi\alpha_{\text{em}}} (\bar{s} \sigma^{\mu\nu} G_{\mu\nu} P_R b)$$

$F_{\mu\nu}$ and $G_{\mu\nu}$ are the QED and QCD Field Strength Tensors

$$O_9 = (\bar{s} \gamma^\mu P_L b)\ (\bar{\mu} \gamma_\mu \mu) \qquad O_{10} = (\bar{s} \gamma^\mu P_L b)\ (\bar{\mu} \gamma_\mu \gamma^5 \mu)$$

The amplitude is given by:

$$\mathscr{A} = \langle\, \gamma(k,\epsilon)\, \mu^+(p_1)\, \mu^-(p_2) \,|\, -\mathscr{H}_{\text{eff}}^{b\to s} \,|\, B_s(p) \,\rangle_{\text{QCD+QED}}$$

$$= -e \frac{\alpha_{\text{em}}}{\sqrt{2}\pi} V_{tb} V_{ts}^* \epsilon_\mu^* \left[ \sum_{i=1}^{9} C_i H_i^{\mu\nu} L_{V\nu} + C_{10} \left( H_{10}^{\mu\nu} L_{A\nu} - i \frac{f_{B_s}}{2} L_A^{\mu\nu} p_\nu \right) \right]$$

The $H^{\mu\nu}$ and $L$ are hadronic and leptonic tensors respectively

# 2. Motivation for introducing the spectral density


- For illustration, consider the contribution from the operators $O_1^{(c)}$ and $O_2^{(c)}$ in the $B \to K\ell^+\ell^-$ decay.
  ($O_{1,2}^{(c)}$ implies either of the two current-current operators.)

$$H^{\mu}(q) = i \int d^4x\, e^{iq\cdot x} < K(\vec{p}_K)|T[J^{\mu}_{\rm em}(x)\, O^{(c)}_{1,2}(0)]|B(\vec{0}\,) > \equiv i \int_{-\infty}^{\infty} dt\, e^{iq_0 t} < K(\vec{p}_K)|T[\tilde{J}^{\mu}_{\rm em}(t,\vec{q}\,)\, O^{(c)}_{1,2}(0)]|B(\vec{0}\,) >$$

- For $t < 0$, the states propagating between $t$ and 0, have $B = 1$ and three momentum $-\vec{q}$. They therefore have energies $> m_B$ and this contribution is real. (Diagram (a))
- For $t > 0$ on the other hand, the states propagating between 0 and $t$ have $B = 0$ (and $S = 1$) and three momentum $\vec{0}$ and therefore can have energies $< m_B$ and therefore a complex contribution. (Diagram (b))

# Motivation for introducing the spectral density (cont)


- For $t > 0$, the correlation function is given by

$$C^{\mu}_{(b)}(t,\vec{q}\,) \equiv \int d^3x\, e^{-i\vec{q}\cdot\vec{x}}\ < K(-\vec{q}\,)|J^{\mu}_{\rm em}(t,\vec{x}\,)\, O^{(c)}_{1,2}(0)|B(\vec{0}\,)> = \int \frac{dE}{2\pi}\, e^{-i(E-E_K)t}\, \rho^{\mu}_{(b)}(E,\vec{q}\,)$$

where

$$\rho^{\mu}_{(b)}(E,\vec{q}\,) = < K(-\vec{q}\,)|J^{\mu}_{\rm em}(0)\,(2\pi)^3\delta^{(3)}(\hat{\mathbf{P}})\,(2\pi)\delta(\hat{H}-E)\,O^{(c)}_{1,2}(0)|B(\vec{0}\,)>$$

- Good news: i) the spectral density $\rho^{\mu}_{(b)}$ is independent of $t$ and is the same in Minkowski and Euclidean space;
  ii) the expression for the correlation function in Euclidean space is the same as above with $e^{-i(E-E_K)t} \to e^{-(E-E_K)t}$;
  iii) the correlation function can be computed in Euclidean space.

- Less good news: The inverse problem of determining the spectral density from the Laplace transform is delicate.

# Motivation for introducing the spectral density (cont.)

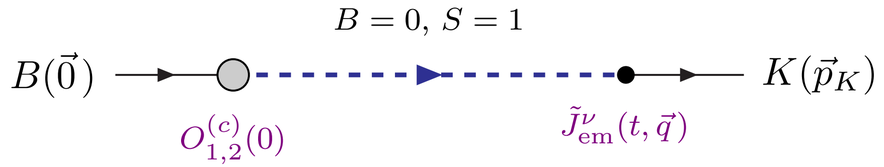


- The hadronic factor in the amplitude from time ordering (b) is:

(b)

$$H^{\mu}_{(b)}(q) = i\int_0^\infty dt\ e^{iq_0 t}\ C^{\mu}_{(b)}(t,\vec{q}\,) = i\int_0^\infty dt\ \int \frac{dE}{2\pi}\ e^{-i(E-E_K-q_0)t}\rho^{\mu}_{(b)}(t,\vec{q}\,) = \lim_{\epsilon\to 0}\int_{E^*}^\infty \frac{dE}{2\pi}\ \frac{\rho^{\mu}_{(b)}(t,\vec{q}\,)}{E-m_B-i\epsilon}$$

($E^* < m_B$ is the threshold energy)

- The HLT method is based on the expansion of the "smearing kernel" in terms of exponentials at **finite** $\epsilon$ :

J.Barata and K.Fredenhagen, (1990)

$$\frac{1}{E-m_B-i\epsilon} \simeq \sum_{n=1}^{N} g_n(m_B,\epsilon)\, e^{-anE}$$ so that

$$H^{\mu}_{(b)}(q) = \lim_{\epsilon\to 0}\sum_{n=1}^{N} g_n(m_B,\epsilon)\int_{E^*}^\infty \frac{dE}{2\pi}\, e^{-aEn}\rho^{\mu}_{(b)}(E,\vec{q}\,) = \lim_{\epsilon\to 0}\sum_{n=1}^{N} g_n(m_B,\epsilon)\, e^{-aE_K n}\ C^{\mu}_{(b),\mathrm{Eucl}}(an,\vec{q}\,)$$

- In principle at least, the $g_n(m_B,\epsilon)$ can be determined and the $C_{(b),\mathrm{Eucl}}(an,\vec{q}\,)$ can be computed so that $H^{\mu}_{(b)}(q)$ can be obtained.

Significant practical issues remain.

# 3. The $B_s \to \mu^+\mu^-\gamma$ Decay Rate at Large $q^2$

R.Frezzotti, **G.Gagliardi,** V.Lubicz, G.Martinelli, CTS, F.Sanfilippo, S.Simula, N.Tantalo, arXiv:2402.03262

- We use this interesting FCNC process to illustrate the elements which we are able to compute without the spectral density approach and to highlight those which require HLT/SFR.
- Preview: The decay rate is dominated by the local form factor $F_V$, but the error estimated from the charming penguin contributions is significant.

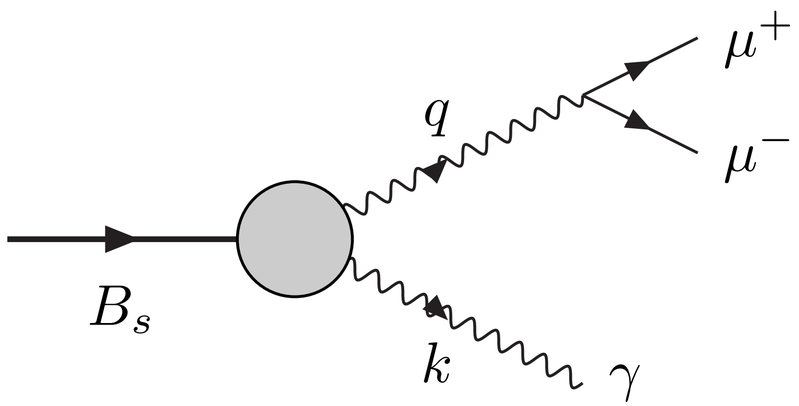


$x_\gamma = \dfrac{2E_\gamma}{m_{B_s}}$, $E_\gamma$ is the energy of the real photon in rest frame of the $B_s$ meson.

$$q^2 = m_{B_s}^2(1 - x_\gamma), \qquad 0 \le x_\gamma \le 1 - \frac{4m_\mu^2}{m_{B_s}^2}$$

- LHCb: $B(B_s \to \mu^+\mu^-\gamma)\,|_{\sqrt{q^2}>4.9\,\mathrm{GeV}} < 2.0 \times 10^{-9}$, arXiv:2108.09283/4

# From the May/June 2024 issue of the Cern Courier

LHCb

# LHCb targets rare radiative decay

Rare radiative b-hadron decays are powerful probes of the Standard Model (SM) sensitive to small deviations caused by potential new physics in virtual loops. One such process is the decay of $B_s^0 \to \mu^+\mu^-\gamma$. The dimuon decay of the $B_s^0$ meson is known to be extremely rare and has been measured with unprecedented precision by LHCb and CMS. While performing this measurement, LHCb also studied the $B_s^0 \to \mu^+\mu^-\gamma$ decay, partially reconstructed due to the missing photon, as a background component of the $B_s^0 \to \mu^+\mu^-$ process and set the first upper limit on its branching fraction to $2.0 \times 10^{-9}$ at 95% CL (red arrow in figure 1). However, this search was limited to the high-dimuon-mass region, whereas several theoretical extensions of the SM could manifest themselves in lower regions of the dimuon-mass spectrum. Reconstructing the photon is therefore essential to explore the spectrum thoroughly and probe a wide range of physics scenarios.

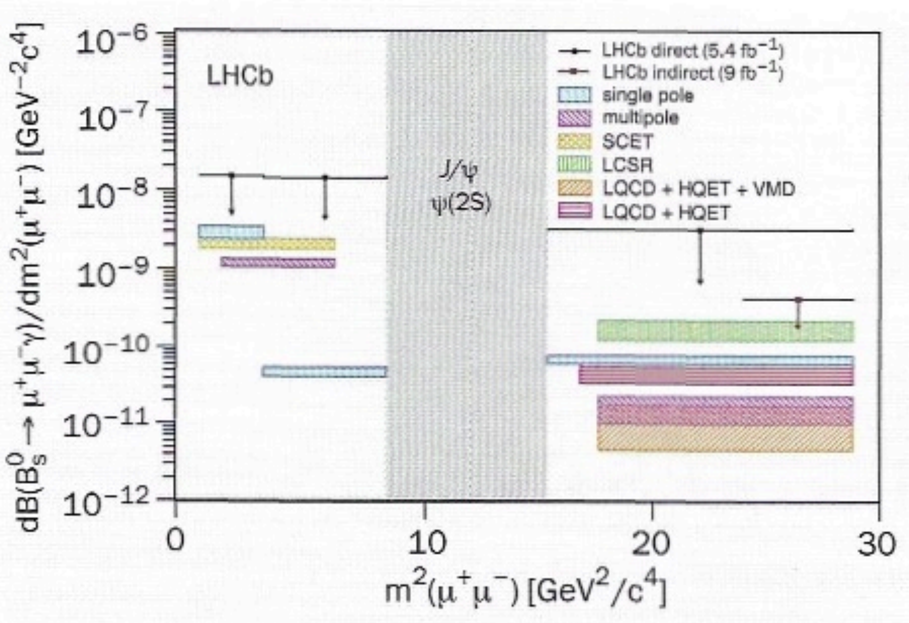


Source: LHCb

**Fig. 1.** *95% confidence limits on differential branching fractions for $B_s^0 \to \mu^+\mu^-\gamma$ in intervals of dimuon mass squared ($q^2$). The shaded boxes illustrate SM predictions for the process, according to different calculations.*

The LHCb collaboration now reports the first search for the $B_s^0 \to \mu^+\mu^-\gamma$ decay with a reconstructed photon, exploring the full dimuon mass spectrum. Photon reconstruction poses additional experimental challenges, such as degrading the mass resolution of the $B_s^0$ candidate and introducing additional background contributions. To cope with this ambitious search, machine-learning algorithms and new variables have been specifically designed with the aim of discriminating the signal among background processes with similar signatures. The analysis ▷

# Reminder of the Effective b → s Hamiltonian

$$\mathscr{H}_{\text{eff}}^{b\to s} = 2\sqrt{2} G_F V_{tb} V_{ts}^* \left[ \sum_{i=1,2} C_i O_i^c + \sum_{i=3}^{6} C_i O_i + \frac{\alpha_{\text{em}}}{4\pi} \sum_{i=7}^{10} C_i O_i \right]$$

$$O_1^c = (\bar{s}_i \gamma^\mu P_L c_j)\ (\bar{c}_j \gamma_\mu P_L b_i) \qquad O_2^c = (\bar{s} \gamma^\mu P_L c)\ (\bar{c} \gamma_\mu P_L b)$$

$$\left( P_{L,R} = \frac{1}{2}(1 \mp \gamma^5) \right)$$

$O_{3-6}$ are QCD Penguins with small Wilson Coefficients

$$O_7 = -\frac{m_b}{e} (\bar{s} \sigma^{\mu\nu} F_{\mu\nu} P_R b) \qquad O_8 = -\frac{g_s m_b}{4\pi\alpha_{\text{em}}} (\bar{s} \sigma^{\mu\nu} G_{\mu\nu} P_R b)$$

$F_{\mu\nu}$ and $G_{\mu\nu}$ are the QED and QCD Field Strength Tensors

$$O_9 = (\bar{s} \gamma^\mu P_L b)\ (\bar{\mu} \gamma_\mu \mu) \qquad O_{10} = (\bar{s} \gamma^\mu P_L b)\ (\bar{\mu} \gamma_\mu \gamma^5 \mu)$$

The amplitude is given by: $\mathscr{A} = \langle \gamma(k,\epsilon)\, \mu^+(p_1)\, \mu^-(p_2) \,|\, -\mathscr{H}_{\text{eff}}^{b\to s} \,|\, B_s(p) \rangle_{\text{QCD+QED}}$

$$= -e \frac{\alpha_{\text{em}}}{\sqrt{2}\pi} V_{tb} V_{ts}^* \epsilon_\mu^* \left[ \sum_{i=1}^{9} C_i H_i^{\mu\nu} L_{V\nu} + C_{10} \left( H_{10}^{\mu\nu} L_{A\nu} - i \frac{f_{B_s}}{2} L_A^{\mu\nu} p_\nu \right) \right]$$

The $H^{\mu\nu}$ and $L$ are hadronic and leptonic tensors respectively

# Contribution from "Semileptonic" Operators - $F_V$ and $F_A$

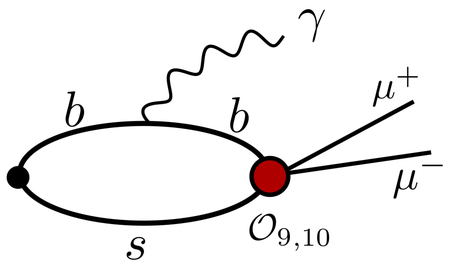


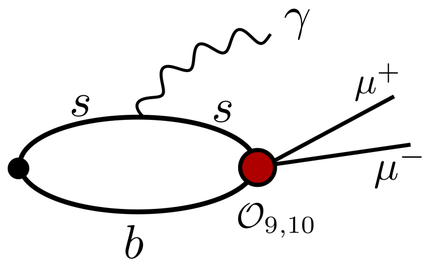


$$H_9^{\mu\nu}(p\,.\,k) = H_{10}^{\mu\nu}(p\,.\,k) = i\int d^4y\ \langle\, 0\,|\,T\big[\,\bar{s}\,\gamma^\nu\,P_L\,b\,(0)\ J^\mu_{\rm em}(y)\big]\,|\,\bar{B}_s(p)\,\rangle$$

$$= -\,i(g^{\mu\nu}\,(k\cdot q) - q^\mu k^\nu)\,\frac{F_A(q^2)}{2m_{B_s}} + \epsilon^{\mu\nu\rho\sigma}\,k_\rho\,q_\sigma\,\frac{F_V(q^2)}{2m_{B_s}}$$

- These form factors can be computed from Euclidean correlation functions (at accessible values of $m_b$).
- We choose $\mathbf{p} = \mathbf{0}$ and $\mathbf{k} = (0,0,k_z)$ and use twisted boundary conditions for $k_z$.
- With such a choice of kinematics: $\dfrac{1}{2k_z}\left(H_V^{12}(p,k) - H_V^{21}(p,k)\right) \to F_V(x_\gamma)$ and $\dfrac{i}{2E_\gamma}\left(H_A^{11}(p,k) + H_A^{22}(p,k)\right) \to F_A(x_\gamma)$.

# The form factors $F_{TV}$ and $F_{TA}$

- In a similar way the following contributions can be computed:

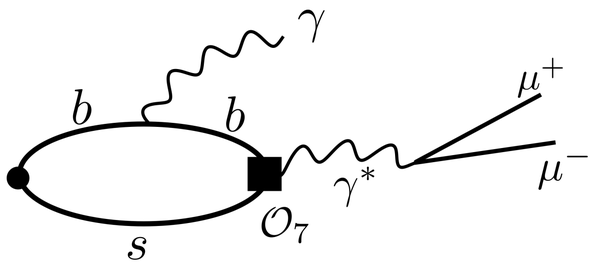


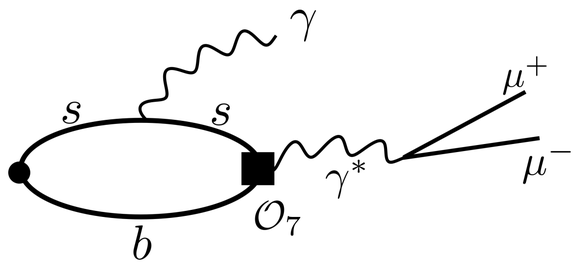


$$H_{7A}^{\mu\nu}(p\,.\,k) = \frac{2m_b}{q^2}\int d^4y \langle\, 0\,|\,T\Big[\,\bar{s}\,\sigma^{\nu\rho}\,P_R\,b\,(0)\;J^{\mu}_{\rm em}(y)\Big]\,|\,\bar{B}_s(p)\,\rangle$$

$$= -\,i(g^{\mu\nu}\,(k\cdot q) - q^{\mu}k^{\nu})\,\frac{m_b F_{TA}(q^2)}{q^2} + \epsilon^{\mu\nu\rho\sigma}\,k_{\rho}\,q_{\sigma}\,\frac{m_b F_{TV}(q^2)}{q^2}$$

- Here, for now, we are isolating the contribution in which it is the virtual photon which is emitted from $O_7$ .

- With our choice of kinematics: $\dfrac{1}{2k_z}\left(H_{TV}^{12}(p,k) - H_{TV}^{21}(p,k)\right) \to F_{TV}(x_\gamma)$ and $\dfrac{-i}{2E_\gamma}\left(H_{A}^{11}(p,k) + H_{A}^{22}(p,k)\right) \to F_{TA}(x_\gamma)$ .

- There is also the useful kinematical constraint that $F_{TV}(1) = F_{TA}(1)$ .

# Numerical Results for $F_V$ , $F_A$ , $F_{TV}$ , $F_{TA}$

- These four form-factors can be computed using “standard” methods at the available heavy quark masses.
- We use gauge field configurations generated by the European Twisted Mass Collaboration (ETMC), with the Iwasaki gluon action and $N_f = 2 + 1 + 1$ flavours of Wilson-Clover light quarks at maximal twist (four ensemble with $0.057\ \text{fm} < a < 0.091\ \text{fm}$).
- We perform the calculations at 5 values of the heavy quark mass corresponding to

$$\frac{m_h}{m_c} = 1, 1.5, 2, 2.5 \text{ and } 3\,,$$

  and at 4 values of $x_\gamma = 0.1,\ 0.2,\ 0.3,\ 0.4$.

- $m_c$ is determined from $m_{\eta_c} = 2.984(4)\ \text{GeV}$.
- Much effort is then devoted to the $m_h \to m_b$ and $a \to 0$ limit, guided by the heavy-quark scaling laws and models for possible resonant contributions.

# Continuum Extrapolation

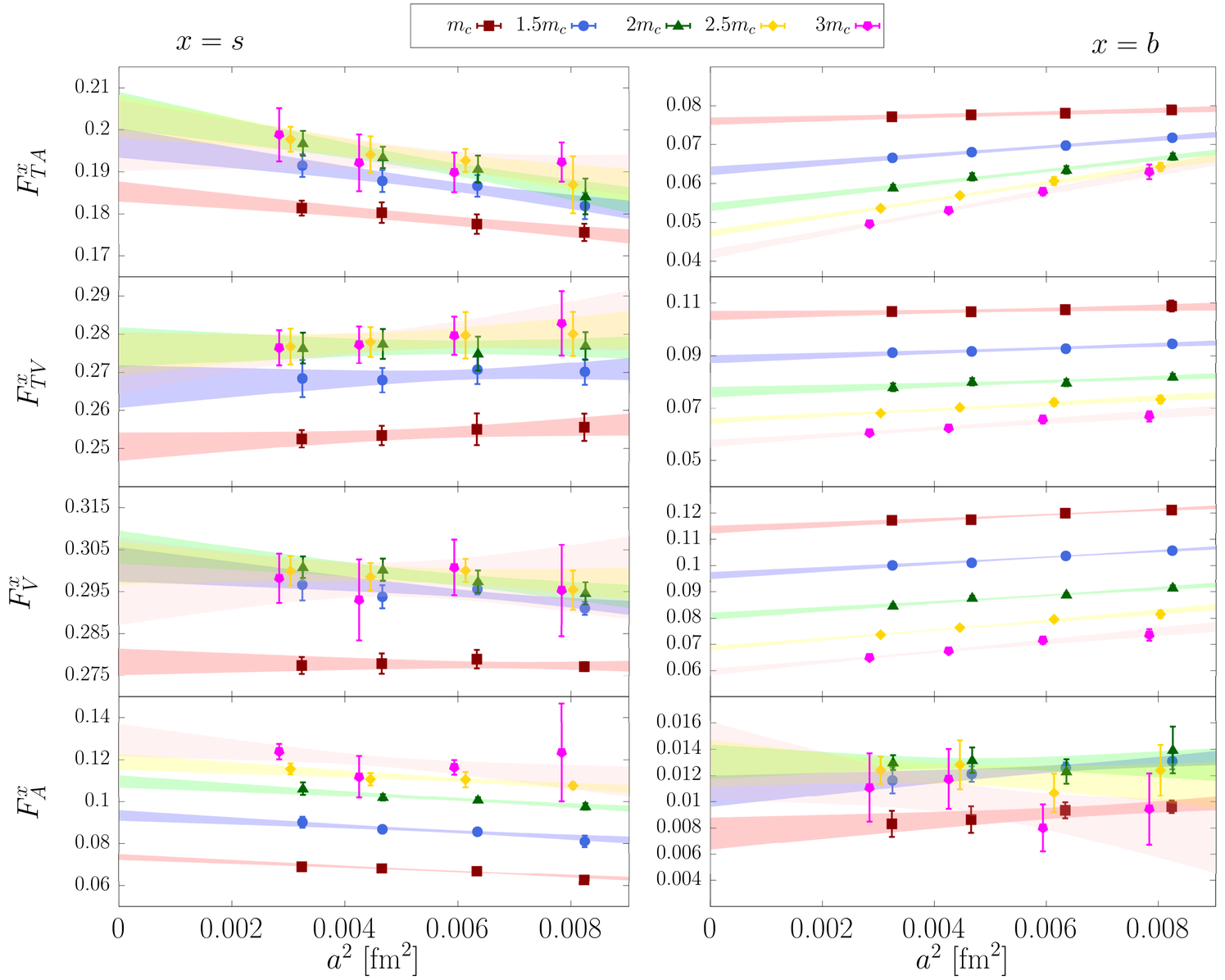


- The continuum extrapolation is performed separately at each value of $m_{H_s}$ and $x_\gamma$ .
- The illustration plots are for $x_\gamma = 0.4$ .

# Extrapolation of the results to $m_{B_s} = 5.367$ GeV

- Having performed the continuum extrapolation, we need to extrapolate the results to the physical value of $m_{B_s}$.
- In the heavy-quark and large $E_\gamma$ limits, scaling laws were derived up to $O(1/m_{H_s}, 1/E_\gamma)$:

M.Beneke and J.Rohrwild, arXiv:1110.3228; M. Beneke, C. Bobeth and Y.-M. Wang, arXiv:2008.12494

$$\frac{F_{V/A}}{f_{H_s}} = \frac{|q_s|}{x_\gamma}\left(\frac{R(E_\gamma,\mu)}{\lambda_B(\mu)} + \xi(x_\gamma, m_{H_s}) \pm \frac{1}{m_{H_s}x_\gamma} \pm \frac{|q_b|}{|q_s|}\frac{1}{m_h}\right) \;;\; \frac{F_{TV/TA}}{f_{H_s}} = \frac{|q_s|}{x_\gamma}\left(\frac{R_T(E_\gamma,\mu)}{\lambda_B(\mu)} + \xi(x_\gamma, m_{H_s}) \pm \frac{1-x_\gamma}{m_{H_s}x_\gamma} + \frac{|q_b|}{|q_s|}\frac{1}{m_{H_s}}\right)$$

- $R(E_\gamma,\mu)$, $R_T(E_\gamma,\mu)$ are radiative correction factors $= 1 + O(\alpha_s)$; $\lambda_B$ is the first inverse moment of the $B_s$-meson LCDA, $\xi(x_\gamma, m_{H_s})$ are power corrections.
- Photon emission from the $b$-quark suppressed relative to the emission from the $s$-quark.
- Tensor form-factors are presented in the $\overline{\text{MS}}$ scheme at $\mu = 5$ GeV.
- However, useful though these scaling laws are, they apply at large $E_\gamma$ (as well as large $m_h$), are there are significant corrections at our lightest values of $m_h$ and smaller values of $E_\gamma$. We therefore us an ansatz which includes the above scaling laws at large $E_\gamma$ as well as VDM behaviour.

# Extrapolation of the results to $m_{B_s} = 5.367$ GeV

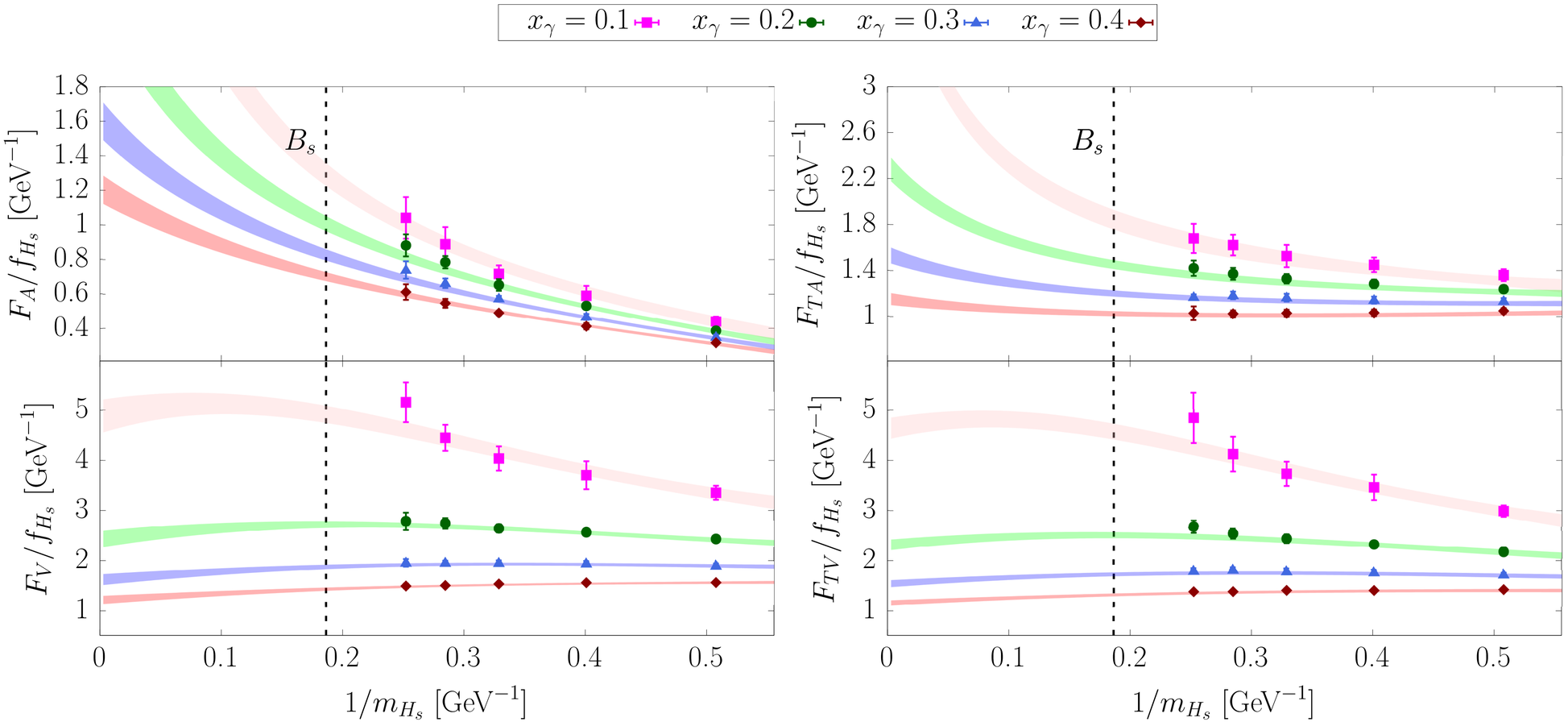

# Comparison with Previous Determinations of the Form Factors

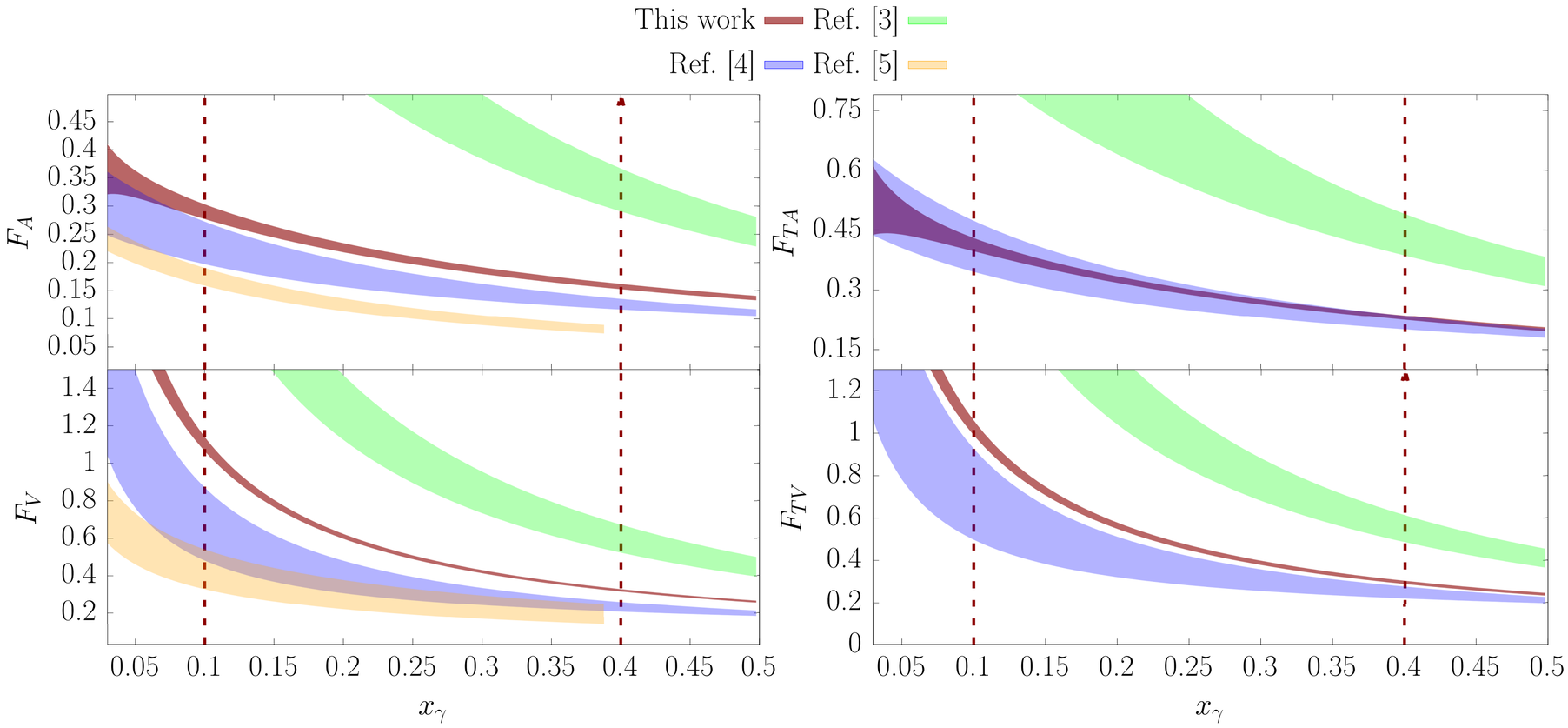


- Ref.[3] = T.Janowski, B.Pullin and R.Zwicky, arXiv:2106.13616, LCSR
- Ref.[4]= A.Kozachuk, D.Melikhov and N.Nikitin, arXiv:1712.07926, relativistic dispersion relations
- Ref.[5]= D.Guadagnoli, C.Normand, S.Simula and L.Vittorio, arXiv:2303.02174, VMD+quark model+lattice at charm

- In general our results for the form factors differ significantly from earlier estimates.

# Other Contributions - $\bar{F}_T$

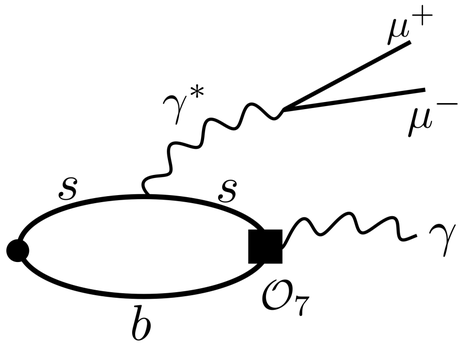


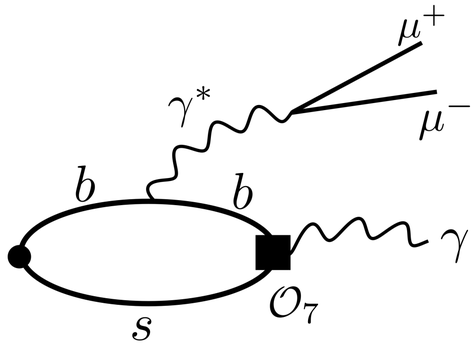


$$H^{\mu\nu}_{\bar{T}}(p,k) = i\int d^4y\; e^{i(p-k)\cdot y}\;\langle\, 0\,|\,T\Big[\,J^{\nu}_{\bar{T}}(0)\;J^{\mu}_{\rm em}(y)\Big]\,|\,\bar{B}_s(\mathbf{0})\,\rangle \equiv -\,\epsilon^{\mu\nu\rho\sigma}\,k_\rho\,p_\sigma\frac{\bar{F}_T}{m_{b_s}}\;\text{ where}$$

$$J^{\nu}_{\bar{T}} = -\,i\,Z_T(\mu)\;\bar{s}\sigma^{\nu\rho}b\;\frac{k^\rho}{m_{B_s}}\;.$$

- The difficulty arises from the first diagram above when $t_y > 0$.
- In that case we potentially have a hadronic intermediate state (e.g. an $s\bar{s}$ $1^-$ state) with smaller mass than $\sqrt{(p-k)^2}$, leading to an imaginary part and problems with the continuation to Euclidean space.

$$\sqrt{m_V^2+E_\gamma^2}+E_\gamma < m_{B_s} \;\Rightarrow\; x_\gamma < 1-\frac{m_V^2}{m_{B_s}^2} \simeq 1-\frac{4m_K^2}{m_{B_s}^2} \simeq 0.96\,.$$

# $\bar{\mathrm{F}}_{\mathrm{T}}$ (cont.)

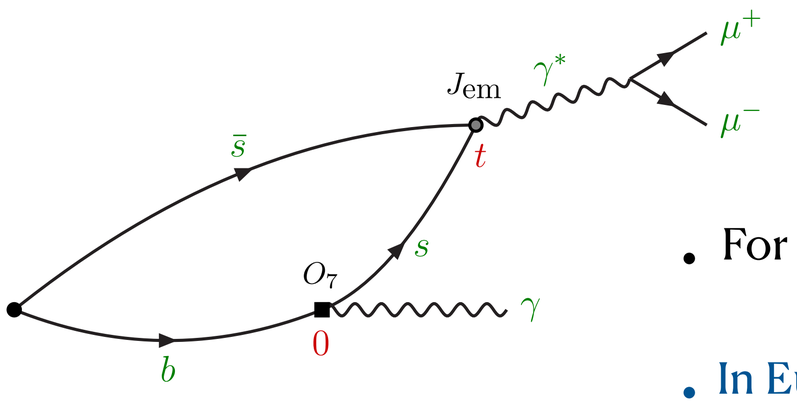


- For $t > 0$ define $C_s^{\mu\nu}(t,\mathbf{k}) \equiv \langle\, 0 \,|\, \tilde{J}^{\mu}_{\mathrm{em},s}(t,-\mathbf{k})\, J^{\nu}_{\bar{T}}(0) \,|\, B_s(\mathbf{0})\rangle \;=\; \displaystyle\int_{E^*}^{\infty} \frac{dE}{2\pi}\, e^{-iEt}\, \rho_s^{\mu\nu}(E,\mathbf{k})\,.$
- In Euclidean space $C_s^{\mu\nu}(t,\mathbf{k}) = \displaystyle\int_{E^*}^{\infty} \frac{dE}{2\pi}\, e^{-Et}\, \rho_s^{\mu\nu}(E,\mathbf{k})\,.$

- For the amplitude we require:

$$H^{\mu\nu}_{\bar{T}_s}(m_B,\mathbf{k}) \;=\; i\int_0^{\infty} dt\; e^{i(m_B-\omega)t}\, C_s^{\mu\nu}(t,\mathbf{k}) \;=\; \lim_{\epsilon\to 0}\int_{E^*}^{\infty} \frac{dE}{2\pi}\, \frac{\rho_s^{\mu\nu}(E,\mathbf{k})}{E-(m_B-\omega)-i\epsilon}\,. \qquad (\omega = |\mathbf{k}|)$$

- Expanding $\dfrac{1}{E-E'-i\epsilon} \simeq \displaystyle\sum_{n=1}^{N} g_n(E',\epsilon)\, e^{-anE}$ we obtain

$$H^{\mu\nu}_{\bar{T}_s}(m_B,\mathbf{k}) \;=\; \lim_{\epsilon\to 0}\int_{E^*}^{\infty} \frac{dE}{2\pi}\, \frac{\rho_s^{\mu\nu}(E,\mathbf{k})}{E-(m_B-\omega)-i\epsilon} \;=\; \lim_{\epsilon\to 0}\sum_{n=1}^{N} g_n(m_B-\omega,\epsilon)\, C_s^{\mu\nu}(an,\mathbf{k})$$

- Now we need to see how well we can make this work.

# $\bar{F}_T$ (cont.)

- Determining the $g_n$ requires a balance between the systematic error due to the approximation of $1/(E - E' - i\epsilon)$ by a finite number of exponentials (in which the coefficients are generally large with alternating signs) and the statistical errors in the correlation functions $C_s(an, \mathbf{k})$.

- We have computed $\bar{F}_T$ at all four values of $x_\gamma$, at three of the five values of $m_h$ ($m_h/m_c = 1, 1.5, 2.5$) and on two of the gauge-field ensembles ($a = 0.0796(1)$ fm and $0.0569(1)$ fm).

  i) $\bar{F}_T$ only gives a very small contribution to the rate and is therefore not needed with great precision.
  ii) The spectral density method is computationally expensive.

- An extrapolation in $\epsilon$ is required, as well as those in $a$ and $m_h$.

- Resulting error is $O(100\%)$ but $\bar{F}_T \ll F_{TV}, F_{TA}$. No clear $x_\gamma$ dependence is observed in our data and we quote:

$$\mathrm{Re}\,\bar{F}_T^s(x_\gamma) = -0.019(19) \text{ and } \mathrm{Im}\,\bar{F}_T^s(x_\gamma) = 0.018(18)\,.$$

# $\bar{F}_T^s$ - Illustrative Plots

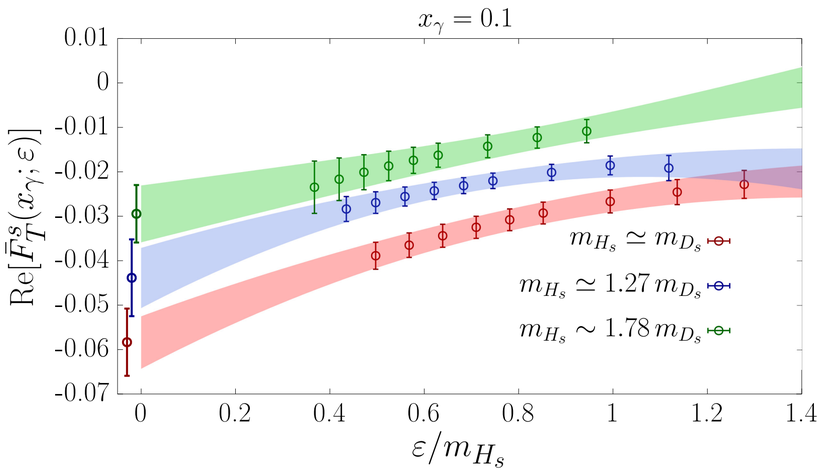


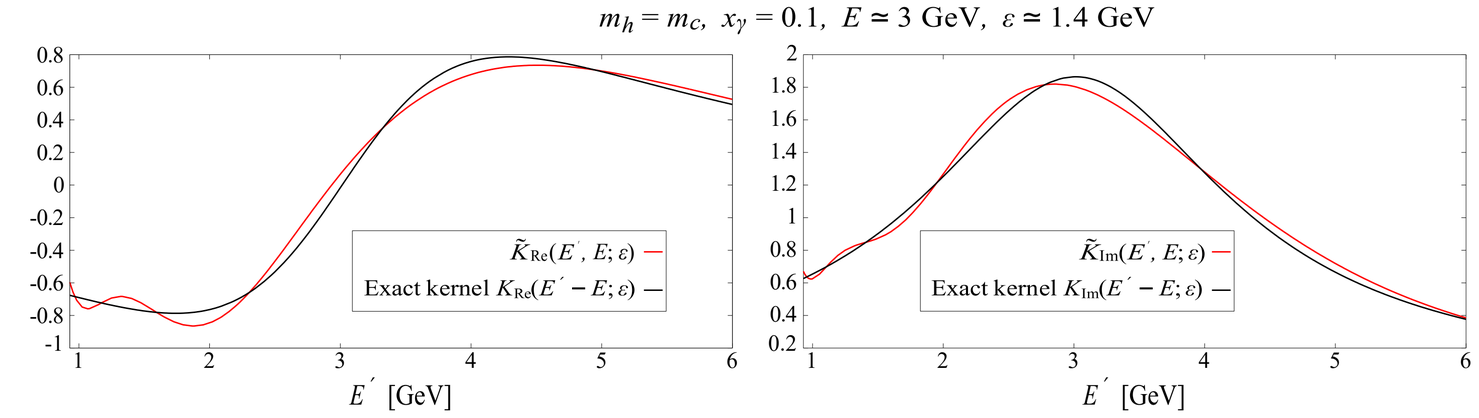


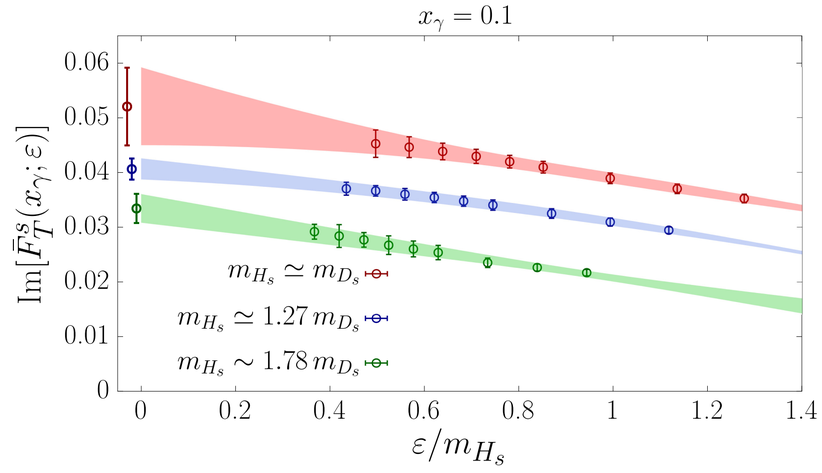


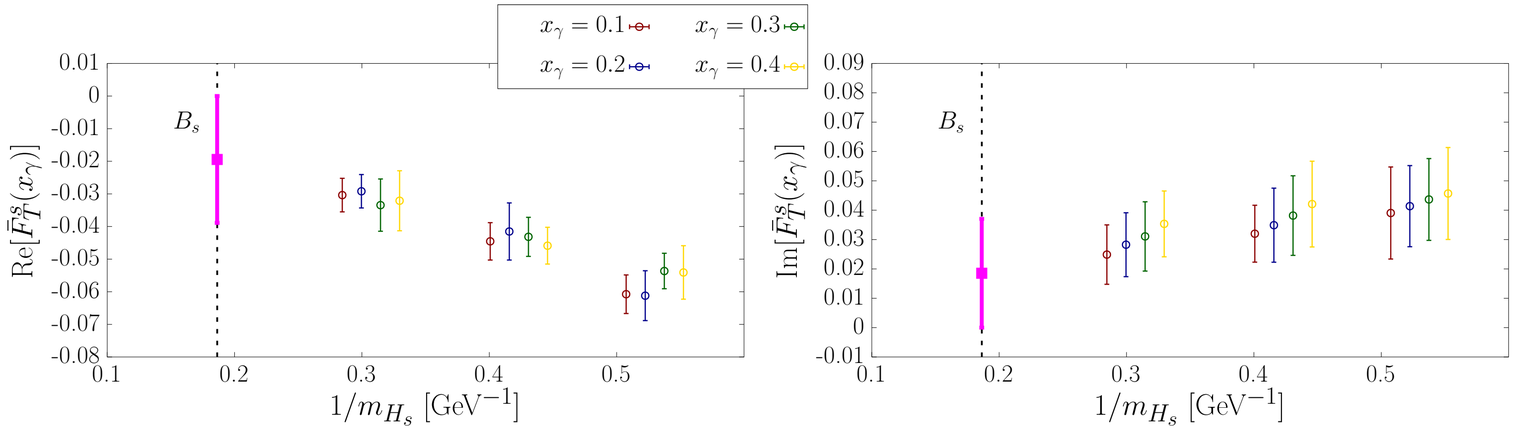

# Other Contributions - Charming Penguins

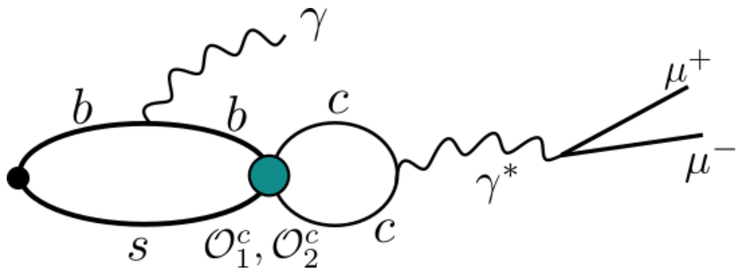


- Of the contributions we have not computed directly , the most significant one at large $q^2$ is expected to be that from the operators $O^c_{1,2}$ (charming penguins) and we are aiming to use the spectral density reconstruction method to overcome this.

- In the meantime we followed previous ideas and estimate the contribution based on VMD inserting all $c\bar{c}$ resonances from the $J/\Psi$ to the $\Psi(4660)$ . It can be viewed as a shift in $C_9 \to C_9^{\text{eff}}(q^2) = C_9 + \Delta C_9(q^2)$ :

$$\Delta C_9(q^2) = -\frac{9\pi}{\alpha_{\text{em}}^2}\left(C_1 + \frac{C_2}{3}\right)\sum_V |k_V| e^{i\delta_V} \frac{m_V \Gamma_V B(V \to \mu^+\mu^-)}{q^2 - m_V^2 + i m_V \Gamma_V}.$$

- $k_V$ and $\delta_V$ parametrise the deviation from the factorisation approximation (in which $\delta_V = k_V - 1 = 0$). We allow $\delta_V$ to vary over $(0,2\pi)$ and $|k_V|$ to vary in the range $1.75 \pm 0.75$ .

# Branching Fractions

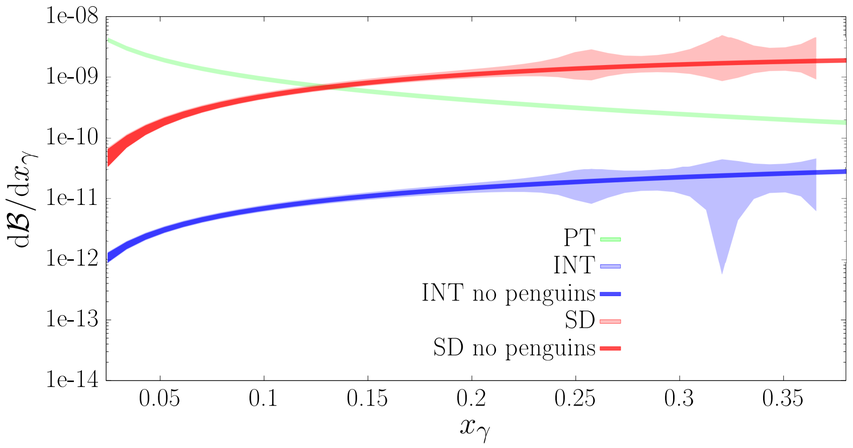


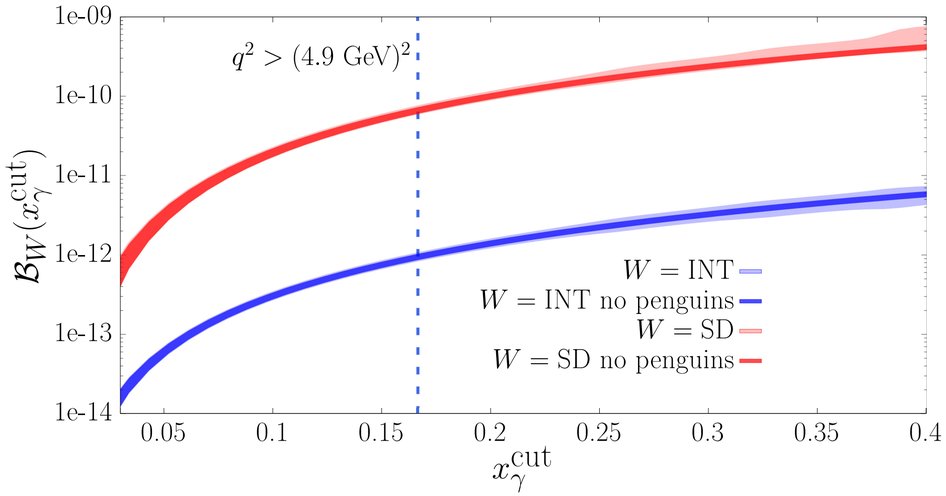


$$\mathcal{B}(x_\gamma^{\mathrm{cut}}) = \int_0^{x_\gamma^{\mathrm{cut}}} dx_\gamma \, \frac{d\mathcal{B}(x_\gamma)}{dx_\gamma}$$

- Structure Dependent (SD) contribution dominated by $F_V$.
- The error from the charming penguins increases with $x_\gamma$ (at $x_\gamma = 0.4$ it is about 30 % ).
- Our Result - $\mathcal{B}_{\mathrm{SD}}(0.166) = 6.9(9) \times 10^{-11}$; LHCb - $\mathcal{B}_{\mathrm{SD}}(0.166) < 2 \times 10^{-9}$.

# Comparisons

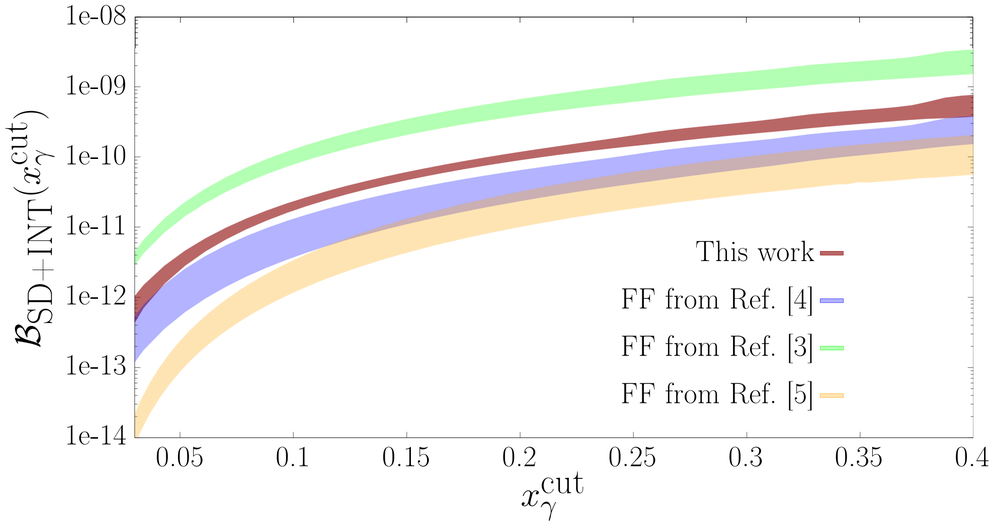


- Ref.[3] = T.Janowski, B.Pullin and R.Zwicky, arXiv:2106.13616, LCSR
- Ref.[4]= A.Kozachuk, D.Melikhov and N.Nikitin, arXiv:1712.07926, relativistic dispersion relations
- Ref.[5]= D.Guadagnoli, C.Normand, S.Simula and L.Vittorio, arXiv:2303.02174, VMD+quark model+lattice at charm
- Discrepancy persists since rate dominated by $F_V$

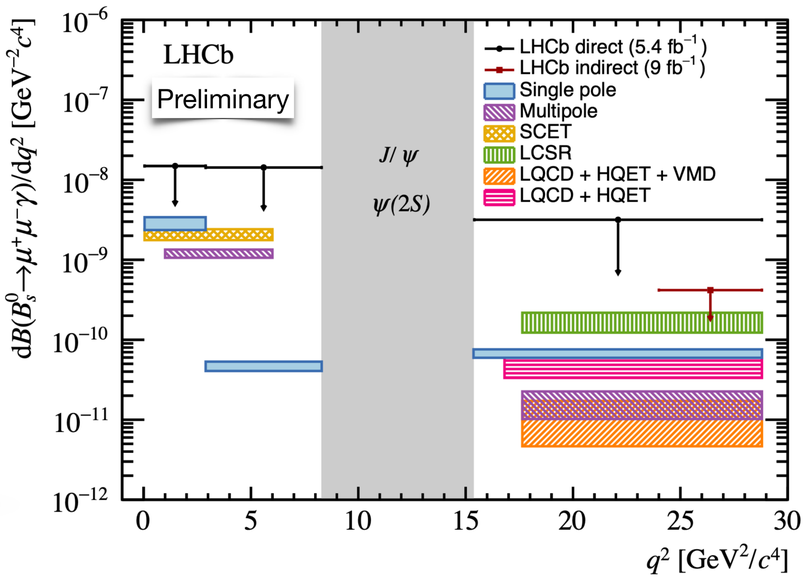


- New LHCb update with direct detection of final state photon.

I.Bachiller, La Thuile 2024
LHCb, 2404.07648

- For $q^2 > 15\ \mathrm{GeV}^2$ the bound is about an order of magnitude higher than before.

# 4. Towards the evaluation of the charming penguin contributions

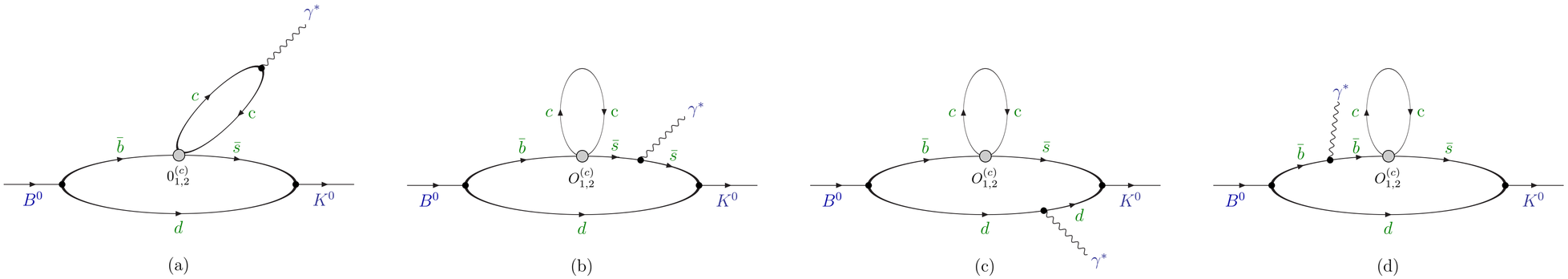


- As explained above, the new spectral density reconstruction techniques, described earlier in this talk, give us the opportunity to evaluate the charming penguin contributions to $B \to K\ell^+\ell^-$ and $\bar{B}_s \to \gamma\mu^+\mu^-$ decays (work in progress).

# Evaluating the charming penguin contributions (cont.)

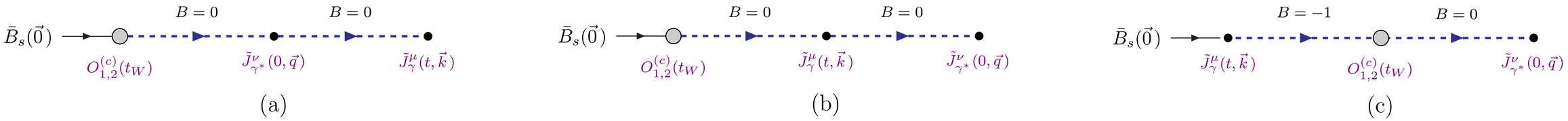


- For $B \to \gamma \ell^+ \ell^-$ decays, with the $B$-meson at rest, the hadronic factor in the amplitude is

$$H^{\mu\nu}_{1,2}(\vec{k}\,) = i \int dt \int d^3x \int dt_W \int d^3y \; \langle 0|T\big[J^{\mu}_{\gamma}(t,\vec{x}\,)\, J^{\nu}_{\gamma^*}(0,\vec{y}\,)\, O^{(c)}_{1,2}(t_W,\vec{0}\,)\big]|\bar{B}_s(\vec{0}\,)\rangle\, e^{ik\cdot x}\, e^{i\vec{k}\cdot\vec{y}}\,,$$

  where the subscripts $\gamma$ and $\gamma^*$ indicate the currents at which the real and virtual photons are emitted.

- There are now three operators and so 6 possible time-orderings. The three above are the ones requiring spectral density methods.

- In (a), $t_W < 0 < t$, on-shell states with energies $E < m_B$ can propagate between $t_W$ and 0.

- In (b), $t_W < t < 0$, on-shell states with energies $E_1 < m_B$ can propagate between $t_W$ and $t$. In addition however, depending on the value of $q$, on-shell states with energies $E_2 < q^0$ can propagate between $t$ and 0. In this case we have a double pole:

- In (c), $t < t_W < 0$, depending on the value of $q$, on-shell states with energies $E < q^0$ can propagate between $t_W$ and 0.

# Evaluating the charming penguin contributions (cont.)

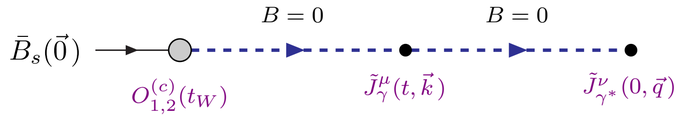


(b)

- For $\bar{B}_s \to \gamma \ell^+ \ell^-$ decays, from diagram (b) we can have a double pole:

$$H^{\mu\nu}_{(b)}(\vec{k}) = -\int_{E_1^*}^{\infty} \frac{dE_1}{2\pi} \int_{E_2^*}^{\infty} \frac{dE_2}{2\pi} \frac{\rho_2^{\mu\nu}(E_1, E_2, \vec{k})}{(E_1 - m_{\bar{B}_s} - i\epsilon)\,(E_2 + k_0 - m_{\bar{B}_s} - i\epsilon)}$$

  - Both factors in the denominator to be expanded in terms of exponentials.

- In the forthcoming paper, we show that in general matrix elements of non-local operators, consisting of $n$ local operators, can be written as a sum of $n!$ spectral integrals each with $n-1$ factors of the form $E_i - E_i' - i\epsilon$ in the denominator.
  - The $E_i$ , $i = 1, \cdots, (n-1)$, are integration variables over the spectral region of energies of channel $i$.
  - The $E_i'$ , are the energies in the $i^{\text{th}}$ channel if energy were conserved at each vertex.
  - As seen previously, not all poles lie in the region of integration, so the corresponding $i\epsilon$ can be dropped (in principle at least)

# 5. Other contributions requiring spectral density methods

- We have already seen that the form factor $\bar{F}_T$ contributing to the $\bar{B}_s \to \gamma \ell^+ \ell^-$ decay amplitude required the spectral density approach.

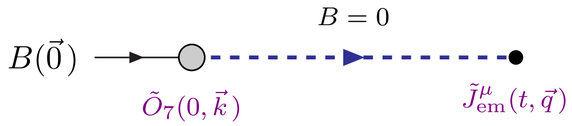


- Although the diagrams are different (e.g. there is no connected charm-quark loop), the above discussion of the charming penguin operators $O^{(c)}_{1,2}$ can be repeated for the chromomagnetic operator $O_8$ . For example:

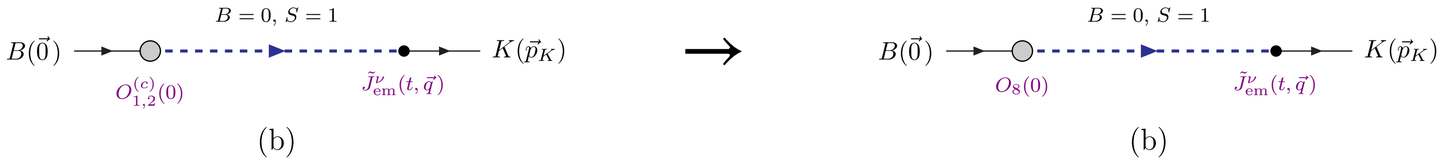


and similarly for $\bar{B}_s \to \gamma \ell^+ \ell^-$ decays.

  - Similarly for the QCD penguins $O_3$- $O_6$ when they are eventually included.

- In general which time orderings require the spectral density approach has to be determined by inspection.

# 6. Renormalisation

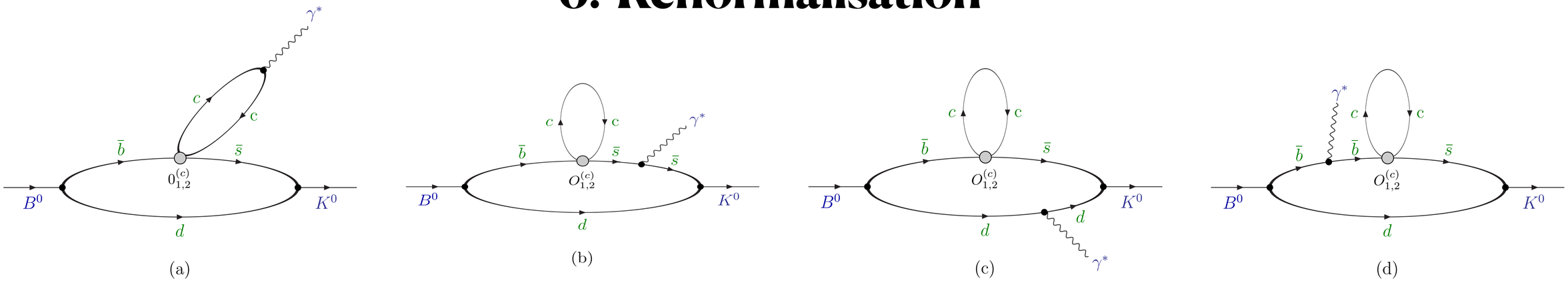


- Renormalisation of the operators is necessary, but highly non-trivial, for the numerical evaluation of the decay amplitudes.
  - The Wilson coefficients are generally computed perturbatively in the $\overline{\text{MS}}$ scheme, which is purely perturbative and in which power UV divergences are not present.
  - Non-perturbative, regularisation independent, schemes exist, which can be used (and which are being widely used) in lattice QCD computations (e.g. RI-Mom, RI-SMom, Schrödinger functional). They then require perturbative matching to the $\overline{\text{MS}}$ scheme to correspond to the known Wilson coefficients.
  - A much more significant problem, is the subtraction of the power divergences, which are present in non-perturbative schemes due to the mixing of the dimension 6-operators $O^{(c)}_{1,2}$ with operators of lower dimension, e.g. $\bar{s}\gamma^5 b$ or $\bar{s}b$.
    - Such divergences appear as inverse powers of the lattice spacing, $1/a^3,\ 1/a^2,\ 1/a$, and must be subtracted non-perturbatively.
    - The divergences, and hence the subtraction procedures, are scheme dependent.
    - In the forthcoming paper we show that the subtractions can be performed for the Twisted Mass formulation of Lattice Fermions being used in the numerical calculations.

# Renormalisation - Contact Terms

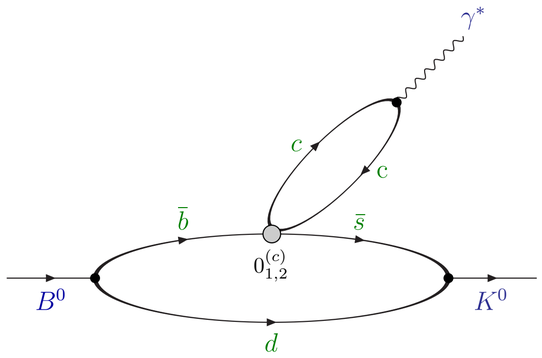

(a)

- When evaluating matrix elements there may be additional UV divergence when two local operators approach each other - contact terms.
- An example is provided by diagram (a) which contains a logarithmic divergence renormalised by subtracting the matrix elements of $O_7$ and $O_9$ with suitable Wilson coefficients.

- However, as we have seen, using SFR we treat the two time orderings separately, and in each case the UV divergence is quadratic as given by dimensional power counting. The quadratic divergences cancel when the two contributions are summed, as required by electromagnetic current conservation.
- In the forthcoming paper we show how to separate the renormalisation of UV divergences (including the cancelation of the power divergences), from the terms which require the SFR/HLT approach.
- Although the details of the separation are process dependent, the approach we follow can be generalised.

# 7. Conclusions

- For $\bar{B}_s \to \gamma \ell^+ \ell^-$ decays, we have computed the local form factors $F_V$, $F_A$, $F_{TV}$ and $F_{TA}$. The amplitude is dominated by $F_V$.
  *There are significant discrepancies with earlier estimates of the form factors obtained using other methods.*

- We have also used HLT & SFR to compute the form factor $\bar{F}_T$. In spite of the $O(100\%)$ error, we confirm that it gives a negligible contribution to the amplitude.

- As $q^2$ is decreased towards the region of charmonium resonances, the uncertainties grow, from 15 % with $\sqrt{q^2_{\rm cut}} = 4.9\,{\rm GeV}$ to about 30 % for $\sqrt{q^2_{\rm cut}} = 4.2\,{\rm GeV}$, largely due to the charming penguins for which we have included a phenomenological parametrisation.

- The priority now is to implement spectral density methods which would allow the evaluation of the charming penguin contributions, as well as those from the operators $O_8$ for $B \to K^{(*)} \ell^+ \ell^-$ and $\bar{B}_s \to \gamma \ell^+ \ell^-$ decays etc..
  Although still in its early stages, this work has begun.

- How to manage the various technical issues optimally will take some effort, but we can confidently expect that such amplitudes will be computed with increasing precision in the coming years.